

Erratum

Probing dark matter caustics with weak lensing[★]

R. Gavazzi^{1,3}, R. Mohayaee², and B. Fort²

¹ Laboratoire d'Astrophysique, UMR 5572 CNRS & Université Paul Sabatier, 14 Av. Edouard Belin, 31400 Toulouse, France
e-mail: rgavazzi@ast.obs-mip.fr

² Institut d'Astrophysique de Paris, UMR 7095 CNRS & Université Pierre & Marie Curie, 98bis Bd. Arago, 75014 Paris, France

³ Oxford University, Astrophysics, Denys Wilkinson Building, Keble Road, Oxford OX1 3RH, UK

A&A, 445, 43–49 (2006), DOI:10.1051/0004-6361:20053557

ABSTRACT

We correct two errors that were present in the former version of this paper. First, a factor 1/3 was missing in the expression of the smooth density profile of the dark matter halo (Eq. (1)) that propagates into the expression of the projected smooth density profile (Eq. (9)). Second, the numerical integration of the caustics' density profile also misses a factor of 2, although the equations are correct. The former error has no effect on the analysis but the latter makes the weak lensing signal twice stronger than previously published. Therefore, the detection of dark matter caustics through weak lensing is made easier. Instead of a superposition of about 200 cluster-size halos, one would require only ~100 such systems for the caustics to show up in ground-based observations. Similarly, space-based weak lensing data would achieve the same detection threshold with ~30 galaxy clusters.

Key words. dark matter – gravitational lensing – errata, addenda

* All erratum is only available in electronic form at
<http://www.edpsciences.org>

Online Material

1. Smooth halo density profile

In Eq. (1) of our original article a factor 1/3 was missing in the expression of the smooth halo density profile as inferred by the self-similar model. Equation (1) should instead read

$$\frac{\rho_{\text{halo}}(\lambda)}{\rho_{\text{H}}} \sim \frac{2.8 \lambda^{-9/4}}{(1 + \lambda^{3/4})^2}. \quad (1)$$

This factor 1/3 is also missing in the approximation of the projected halo density profile (Eq. (9) in the previous version). It then reads:

$$\Sigma_{\text{halo}}(\lambda) \simeq r_{\text{ta}} 7.56 \lambda^{-5/4} \rho_{\text{H}}. \quad (2)$$

Therefore the only consequences of this error for the remainder of the paper is that the smooth black solid curves of Fig. 1 (previous version) should now look like Fig. 1 here (both are lowered by a factor 1/3).

2. Caustics density profile and weak lensing

In addition, when we numerically integrated the density profile of caustics in order to infer their projected counterpart, an extra factor 2 was also missing (the leading factor 2 of Eq. (8) lacking in the numerical integration algorithm). Although all the remaining equations are correct, the weak lensing signal strength is thus increased by this extra factor of 2. In this erratum note Figs. 2 and 3 account for this change. Moreover, we took advantage of this erratum to improve the plotting quality of Fig. 3.

3. Consequences

The increased shear signal translates into a gain in the number of systems that need to be stacked to achieve a significant detection of dark matter caustics. The signal-to-noise ratio is straightforwardly changed by the same factor of 2.

Let us first consider the ideal case in which we have perfect knowledge of the virial (or turnaround) radius of every stacked halo. The required number of cluster-size halos is lowered to $N \sim 50$. If the dark matter temperature is non zero, with $N = 100$ (resp. 250) clusters, one could achieve a limit $\sigma < 170 \text{ km s}^{-1}$ (resp. 40 km s^{-1}) at a 95% confidence level. If one considers galaxies instead of cluster-size haloes, the number of such systems to be stacked is divided by two in the same way. For space-based weak lensing observations, the factor of ~ 3 gain in sensitivity is conserved.

If we now turn back to the realistic situation in which the virial radius of individual clusters is known with a $\sim 3\text{--}10\%$ accuracy, the results are also changed in the same way. One now needs only ~ 200 stacked clusters to be observed both in weak lensing and X-ray.

To conclude, the main changes due to the errors present in the previous version make the possibility of detecting dark matter caustics even less challenging.

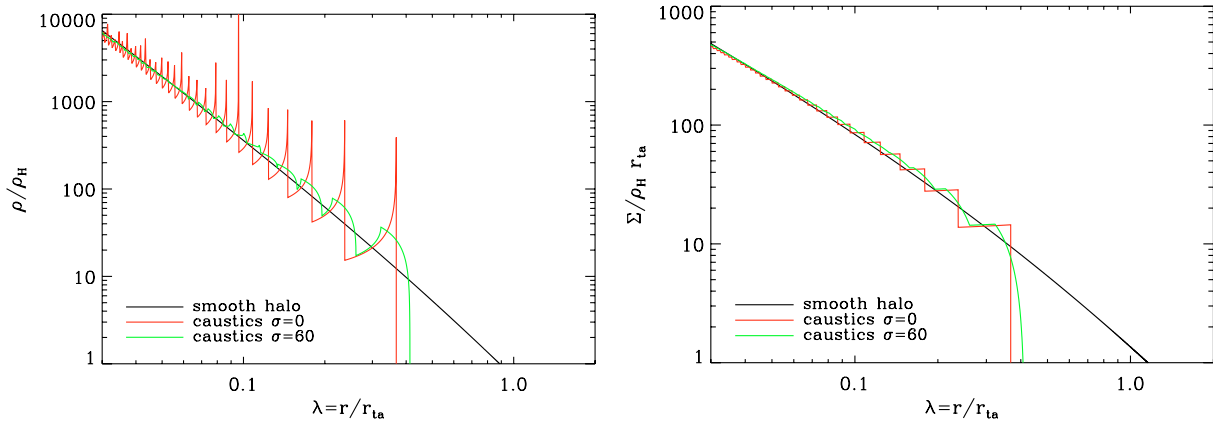


Fig. 1. *Left panel:* tridimensional density profile for the halo (black), for the caustics in a perfectly cold medium (red) and for the caustics smoothed out by a warm/hot dark matter with velocity dispersion $\sigma = 60 \text{ km s}^{-1}$ (green). Densities are expressed in units of the background density ρ_H . Red spikes are all singular with infinite density and limited here to finite values because of finite resolution. *Right panel:* the same colour-coding for the projected 2D density profiles in units of $\rho_H r_{ta}$. When projected, caustic peaks are smoother and look like a flight of stairs. Therefore, we expect low lensing magnifications close to the caustics.

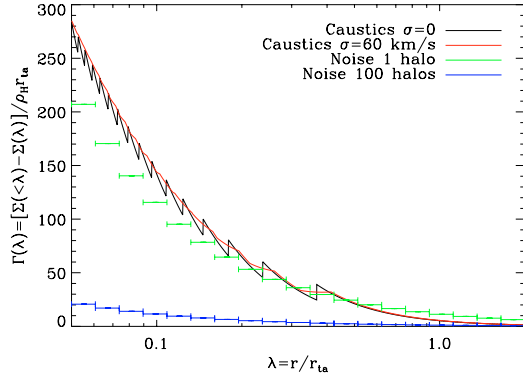


Fig. 2. $\Gamma(\lambda)$ contribution of caustics for two values of σ : cold medium $\sigma = 0$ (black curve) and warm medium $\sigma \sim 60 \text{ km s}^{-1}$ (red curve). The green (resp. blue) “binned” curve is the noise level for one (resp. 100 stacked) halo(s).

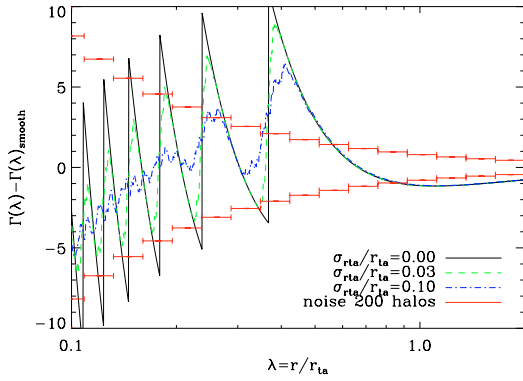


Fig. 3. Difference between the $\Gamma(\lambda)$ contribution of cold caustics and the smooth component. We illustrate the blurring effect of an imperfect knowledge of the turnaround radius of stacked halos. The solid black line, dashed green line, and dot-dashed blue line correspond to zero, 3%, and 10% uncertainties, respectively. As in Fig. 2, the binned curve represents the noise level achieved with 200 stacked halos. The convolution effect of error in the assumed/measured value of r_{ta} is important and a significant detection of caustics requires well-determined turnaround radii (\lesssim a few percents relative accuracy). The very small-scale wiggles in the plot are numerical artifacts and ideally the only sawtooth patterns are those due to caustics.